THE ASTROPHYSICAL JOURNAL, 429:545–553, 1994 July 10

NONPOLYTROPIC MODEL FOR THE COMA CLUSTER

R. FUSCO-FEMIANO
Istituto di Astrofisica Spaziale, C.N.R., C.P. 67, 00044 Frascati, Italy
AND
JOHN P. HUGHES
Harvard-Smithsonian Center for Astrophysics, 60 Garden Street, Cambridge, MA 02138
Received 1992 July 27; accepted 1994 January 6

ABSTRACT

In this article we demonstrate, for the first time, how a physically motivated static model for both the gas and galaxies in the Coma Cluster of galaxies can jointly fit all available X-ray and optical imaging and spectroscopic data. The principal assumption of this nonpolytropic model (Cavaliere & Fusco-Femiano 1981, hereafter CFF), is that the intracluster gas temperature is proportional to the square of the galaxy velocity dispersion everywhere throughout the cluster; no other assumption about the gas temperature distribution is required. After demonstrating that the CFF nonpolytropic model is an adequate representation of the gas and galaxy distributions, the radial velocity dispersion profile, and the gas temperature distribution, we derive the following information about the Coma Cluster:

1. The central temperature is about 9 keV and the central density is 2.8×10^{-3} cm^{-3} for the X-ray emitting plasma;
2. The binding mass of the cluster is approximately 2×10^{15} $M_\odot$ within 5 Mpc (for $H_0 = 50$ km s^{-1} Mpc^{-1}), with a mass-to-light ratio of ~ 160 $M_\odot/L_\odot$;
3. The contribution of the gas to the total virial mass increases with distance from the cluster center, and we estimate that this ratio is no greater than $\sim 50\%$ within 5 Mpc.

The ability of the CFF nonpolytropic model to describe the current X-ray and optical data for the Coma Cluster suggests that a significant fraction of the thermal energy contained in the hot gas in this as well as other rich galaxy clusters may have come from the interaction between the galaxies and the ambient cluster medium.

Subject headings: galaxies: clustering — intergalactic medium — X-rays: galaxies

1. INTRODUCTION

Polytropic intracluster gas distributions were introduced by Lea (1975), Gull & Northover (1975), and Cavaliere & Fusco-Femiano (1976). In these models, ignorance about the complex history of the intracluster medium (ICM) is parameterized by a single quantity: the polytropic index γ, which relates the gas density and temperature distributions through $T \sim \rho^{\gamma-1}$. The inequality $\gamma < 5/3$ corresponds to stability against convection, and the value $\gamma = 5/3$ represents the adiabatic distribution. In the limit of an isothermal distribution ($\gamma = 1$) one obtains the hydrostatic isothermal-β model, where the X-ray surface brightness at a projected radius b has an analytical expression given by

$$S(b) = S(0)[1 + (b/R_c)^2]^{-3\beta+1/2} .$$

Here R_c is the core radius, and β is the ratio of the specific energy density of the galaxies and gas (Cavaliere & Fusco-Femiano 1976) expressed as $\beta = \mu m_H \sigma^2/kT$, where σ is the galaxy line-of-sight velocity dispersion and T is the isothermal gas temperature. This relation has been used successfully to fit the X-ray surface brightness emission from numerous clusters of galaxies (Gorenstein et al. 1978; Branduardi-Raymont et al. 1981; Abramopoulos & Ku 1983; Jones & Forman 1984).

In contrast to the X-ray surface brightness distributions of clusters, information on the temperature distribution has been more difficult to obtain due to technical limitations of instrumentation flown on past X-ray astronomy satellites. The Coma Cluster is one of the few clusters for which there is some knowledge of the temperature distribution. Direct X-ray spectral observations (Watt et al. 1992) have shown that the core of the Coma Cluster is very nearly isothermal out to roughly 30′. Other X-ray spectral data, however, obtained from mechanically collimated instruments with fields of view from 45′ to 3°, which examined larger regions of the Coma Cluster than did Watt et al., strongly require a radially decreasing temperature distribution in the cluster atmosphere.

As was first pointed out by Hughes et al. (1988b), self-consistent polytropic models were unable to provide acceptable fits to the X-ray imaging and spectral data on Coma. These authors introduced an ad hoc hybrid model consisting of a central isothermal region surrounded by a polytropic distribution which did yield acceptable fits. This model was motivated by theoretical considerations of the effects of electron heat conduction on the intracluster gas which would occur most rapidly in the central region of a cluster where the electron densities were the highest. Recently David, Hughes, & Tucker (1992) studied the evolution of gas in a cluster of galaxies in the presence of significant electron heat conduction using a hydrodynamical simulation. They found that a large, nearly isothermal central region would develop for values of thermal conductivity between about 0.1 and full Spitzer conductivity. This model was also able to describe eight present-day observed properties of the gas distribution in the Coma Cluster: the central gas density, the slope of the surface brightness profile at large radii, and several observed temperatures.

However, neither of these models was able to make a prediction about the distribution or dynamics of the cluster member galaxies.

In this paper we take a different approach from David et al. (1992). Instead of proposing specific mechanisms for energy input to or transport throughout the intracluster medium, we examine a static model which is really just a generalization of the earlier polytropic models. This new model, originally proposed by Cavaliere & Fusco-Femiano (1981, hereafter CFF), retains the most successful feature of the old polytropic models (that is, the description of the X-ray surface brightness distribution) but allows for the possibility that both the gas temperature and galaxy velocity dispersion distributions are not isothermal. In this new model, which we refer to as the CFF nonpolytropic model, although the temperature and velocity dispersion are functions of radius, they are still related to each other through the parameter β (see equation [1] below).

Unlike previous polytropic models, a solution to the CFF nonpolytropic model requires us to define an explicit form for the gravitational potential of the cluster. In principle, the choice of this function could be arbitrary, although in practice, even for a cluster as well studied as Coma, the current X-ray and optical data are unable to set strong limits on the shape of the underlying gravitational potential (see, for example, Hughes 1989). For simplicity we have assumed that the virial mass follows a King (1966) isothermal sphere model and that the galaxies are distributed like the virial mass. These assumptions allows us to derive self-consistent solutions for the gas and galaxy density distributions, as well as the gas temperature and velocity dispersion profiles, for comparison with observed data.

The slow radial decrease of both the velocity dispersion and gas temperature profiles for the Coma Cluster qualitatively support the model. The purpose of our article is to demonstrate quantitative agreement with the available data on this cluster. Specifically, we examine the X-ray surface brightness data from the *Einstein* imaging proportional counter (IPC) (Hughes et al. 1988b), the spectral data obtained by the X-ray satellites *Tenma* (Hughes et al. 1988b), *EXOSAT* (Hughes, Gorenstein, & Fabricant 1988a), and *Ginga* (Hughes et al. 1993), and the optical velocity dispersion profile and galaxy density distributions (The & White 1986). We determine best-fit values and errors for the various model parameters. The paper is organized as follows. In § 2 we discuss the features of the CFF nonpolytropic model. The fits to the IPC and spectral data are in §§ 3 and 4, respectively. Section 5 reports the fits to the optical data. Discussion of the cluster binding mass implied by the model appears in § 6, and the conclusions are in § 7.

2. THE CFF NONPOLYTROPIC MODEL

The scope of this work is to verify whether the available X-ray and optical data can be described by means of the static model, originally formulated by CFF, in which the heating of the ICM is controlled by local conditions. In particular, we consider the case where the relation

$$kT(R) = \mu m_{\rm H}\, \sigma^2(R)/\beta \qquad (1)$$

holds everywhere throughout the cluster.

This model was originally formulated starting from the constraint that a reasonable fraction of the gas may have come from stars in cluster galaxies, as indicated by the observed metallicity of the intracluster gas (Mitchell et al. 1976; Serlemitsos et al. 1977; Mitchell & Culhane 1977). Early studies (Larson & Dinerstein 1975; De Young 1978) showed that the energy input from a population of supernovae, which yielded the observed iron abundance might be efficiently converted to bulk kinetic energy of the gas and then thermalized to temperatures consistent with the continuum X-ray measurements. The kinetic energy of the ejected gas, initially moving at the galaxy's speed with respect to the cluster center of mass, would be degraded into internal energy by collisions with the ambient intracluster gas. On average, this heating mechanism should give a temperature of the order of $kT \sim \sigma^2$, neglecting any additional energy input to the gas due to the ejection process itself (White 1991).

More recent scenarios for the evolution of the ICM have changed this picture slightly. It is now known that, although some of the intracluster gas must have been injected by the member galaxies to account for the observed metallicities, most of the ICM must be primordial, since the gas mass is much greater than the observed stellar mass of the cluster galaxies (Blumenthal et al. 1984; Davis et al. 1990). During the gravitational collapse of the cluster, this primordial gas would have been compressed and heated by processes different from those which would have heated the galaxies. In addition, simulations of cluster formation indicate that the galaxy velocity anisotropy should vary with radius, which would appear to make it unlikely for equation (1) to be strictly correct throughout the cluster. Nevertheless, the heating of the ICM is a very complex issue, and thus testing the assumptions implicit in the CFF nonpolytropic model against actual cluster data is a valuable excercise.

Inserting equation (1) into the equation that governs the equilibrium condition for the gas and the galaxies in the same potential well,

$$\mu m_{\rm H}\, n/\rho_G = dp/dp_G\,,$$

it is possible to obtain the general expression for the gas density,

$$n/n_0 = (\rho_G/\rho_{G_0})^{\beta}(\sigma^2/\sigma_0^2)^{\beta-1}\,, \qquad (2)$$

where n is the gas density, ρ_G is the galaxy density, and $p_G = \rho_G \sigma^2$. Central values of quantities are designed with subscript 0.

An explicit expression is obtained using definite relationships $\sigma = \sigma(W)$ and $\rho_G = \rho_G(W)$, where W is the normalized gravitational potential $[W(R) = G\int_R^{R_t} M(r) r^{-2}\sigma^{-2}\,dr]$. The cluster boundary, R_t, is defined to be the radius where $\rho_G = \sigma = 0$.

The velocity dispersion of the Coma Cluster is observed to decrease with increasing projected distance from the cluster center (Rood et al. 1972; Kent & Gunn 1982; Kent & Sargent 1983; The & White 1986). One of the possible functions consistent with such a monotonic decrease is a King (1966) isothermal sphere, which gives for the velocity dispersion,

$$\frac{\sigma^2}{\sigma_0^2} = \frac{I_{5/2}(W)}{I_{5/2}(W_0)}\,\frac{I_{3/2}(W_0)}{I_{3/2}(W)}\,, \qquad (3)$$

and for the galaxy density,

$$\rho_G/\rho_{G_0} = e^{W-W_0} I_{3/2}(W)/I_{3/2}(W_0)\,,$$

where

$$I_q(W) = \int_0^W e^{-\eta}\eta^q\,d\eta$$

is the incomplete gamma function $\gamma(q+1, W)$.

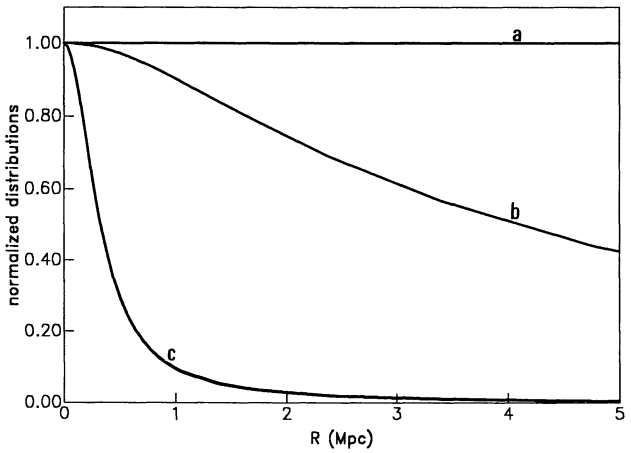

FIG. 1.—Temperature normalized distributions for the isothermal β-model (*a*) and the CFF nonpolytropic model (*b*). Density normalized distribution (c) for both the models.

In turn, $W(R)$ is derived from the full Poisson equation that includes the total density $\rho(W) = n(W) + \rho_G(W)$ (we include in ρ_G any "virial mass" distributed like the galaxies) (King 1966; Cavaliere & Fusco-Fermiano 1978). According to relation (1), the temperature distribution is given by equation (3).

In this model the relevant parameters, which are to be determined by fits to the X-ray and optical data, are the following: n_0, the central gas density; T_0, the central gas temperature; R_c, the core radius of the galaxy space distribution; W_0, the central value of the normalized gravitational potential; and β, the ratio of the specific energy between the galaxies and gas. The X-ray imaging and spectral data can be analyzed separately due to the limited energy bandwidth of the IPC (0.5–4 keV) and the very limited spatial resolution of the higher energy spectrometers. The imaging data put constraints on the allowed values for β and R_c, while the spectral data constrain T_0 and W_0. The optical data are most sensitive to W_0. Normalizations to the imaging and spectral data permit us to derive the central gas density n_0.

The expression that allows computation of the cluster binding mass is derived by combining the spherically symmetric condition of hydrostatic equilibrium with the ideal gas law:

$$\frac{kT}{\mu m_H}\left(\frac{dn}{n}+\frac{dT}{T}\right) = -\frac{GM(R)}{R^2}\,dR\,,$$

which may be written as

$$M(y) = \frac{kTR_c}{\mu m_H G}\left(\frac{dn}{n\,dW}+\frac{dT}{T\,dW}\right)y^2\,\frac{dW}{dy}\,,$$

where $y = R/R_c$. For the CFF nonpolytropic model, the derivatives assume the following forms:

$$\frac{dn}{n\,dW} = \beta + (\beta - 1)\,\frac{e^{-W}W^{5/2}}{I_{5/2}(W)} + \frac{e^{-W}W^{3/2}}{I_{3/2}(W)}\,,$$

$$\frac{dT}{T\,dW} = e^{-W}\,\frac{I_{3/2}(W)W^{5/2} - I_{5/2}(W)W^{3/2}}{I_{3/2}(W)I_{5/2}(W)}\,.$$

The gravitational gradient dW/dy is given by the solution of the full Poisson equation (Cavaliere & Fusco-Femiano 1978).

Figure 1 shows the radial temperature and density distributions (normalized by their central values), which are solutions of the CFF nonpolytropic model. The radial distributions from the isothermal-β model are also shown for comparison.

3. SPATIAL ANALYSIS

The IPC on the *Einstein Observatory* (Giacconi et al. 1979) produced an extensive set of imaging X-ray data on the Coma Cluster. These data were analyzed by Hughes et al. (1988b), and initial reduction procedures are given there. Pointings were made in a number of locations but not in a uniform manner, and since the X-ray image of Coma is distinctly elliptical, it was not possible to obtain a properly averaged radial surface brightness profile from the existing set of images. In this paper, we use the so-called north data set, where the spatial coverage of the cluster was most complete and extended to a radius of roughly 40′ from the cluster center. We have also considered the surface brightness profile composed of data from all the fields (see Hughes 1989), and, although numerical values change somewhat when this data set is used, our conclusions are not modified.

Model surface brightness profiles were determined by calculating the density and temperature as a function of radius from the expressions in § 2 and projecting the quantity $n^2\Lambda(T)$ to the line of sight. To calculate $\Lambda(T)$, the intrinsic emissivity of the gas as seen by the IPC, we needed to assume a value for the distance (140 Mpc), the column density of interstellar absorbing matter in the direction to Coma (3×10^{20} cm^{-2}), and the metal abundance (25%). The convolution of an X-ray spectrum at temperature T generated in conjunction with the preceding parameters with the effective area, and spectral response of the IPC then yielded $\Lambda(T)$. We used the Raymond & Smith (1977; also J. Raymond 1993, private communication) plasma emission model throughout this work. To approximate the spatial response of the IPC, model surface brightness profiles are convolved with a circular Gaussian ($\sigma = 0.6$). The IPC data were most constraining of parameters β, R_c, and n_0, while only a lower bound on the value of W_0 was obtained (see Table 1 and Fig. 8). Because of the limited energy bandwidth of the IPC, the surface brightness data are quite insensitive to the value of T_0, and so we set it to a value of roughly 9 keV and keep it fixed. Varying the central temperature by as much as 20% introduced less than about a 2% change in the best-fit values of β and R_c.

Figure 2 shows the X-ray surface brightness of the Coma Cluster for the data from the northern region, along with the best-fit nonpolytropic model. The best-fit parameter values and the χ^2 value, reported in Table 1 with 90% confidence level errors (single parameter, $\chi^2_{\rm min} + 2.71$), are very similar to those obtained with the isothermal β-model (from Hughes et al. 1988b and reproduced in col. [3] of Table 1). As shown in

TABLE 1

BEST-FIT SPATIAL PARAMETER VALUES FOR COMA CLUSTER

Parameter (1)	Nonpolytropic model (2)	Isothermal β-Model[a] (3)
R_c	$8.'1(+0.'8; -1.'0)$	$7.'6 \pm 0.'7$
β	$0.644(+0.032; -0.050)$	0.63 ± 0.03
$n_0(\times 10^{-3}$ cm$^{-3})$[b]	$2.77(+0.26; -0.20)$	2.6 ± 0.3
W_0	$9.6(\ldots; -2.4)$[c]	...
χ^2(dof)	13.1 (17)	12.8 (18)

[a] Hughes et al. 1988b.
[b] $H = 50$ km s^{-1} Mpc^{-1}.
[c] Indeterminate error bound.

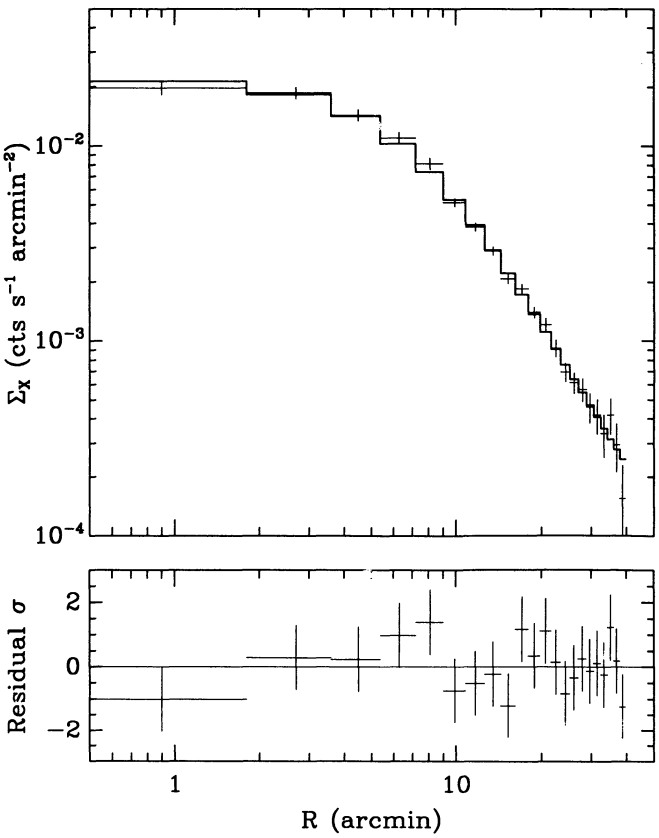

FIG. 2.—Radially averaged IPC X-ray surface brightness of the Coma Cluster with best-fit nonpolytropic model.

Figure 1, the density profile of the CFF nonpolytropic model is virtually indistinguishable from that of the isothermal β-model; $n/n_0 = (\rho_G/\rho_{G0})^{\beta}$. This is due to the slow radial decrease of the galaxy velocity dispersion (see eq. [2] and Fig. 6*a*). The slight difference in χ^2 values between the two models is presumably due to the use of the King model approximation, i.e., $n(R)/n_0 = [1 + (R/R_c)^2]^{-3\beta/2}$, in the work of Hughes et al. 1988b.

Figure 3 presents the results of fits for β and R_c in the form of two-dimensional χ^2 contours (68% and 90% confidence levels

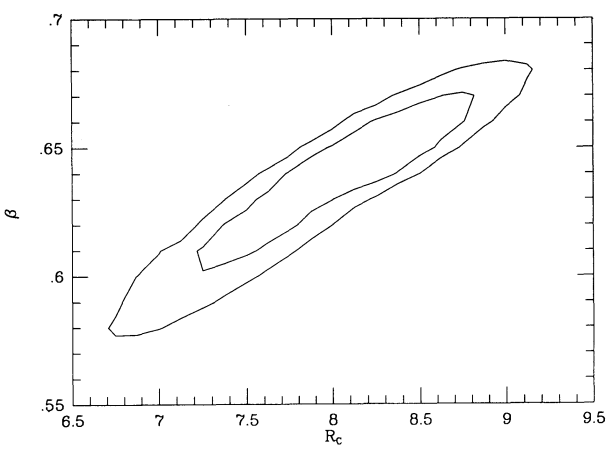

FIG. 3.—Results of fits to the spatial data. Two-dimensional χ^2 contours (at the 68% and 90% confidence levels) for β vs. R_c using the CFF nonpolytropic model.

with $\chi^2_{min} + 2.3$ and $\chi^2_{min} + 4.61$, respectively; see Avni 1976; Lampton, Margon, & Bowyer 1976). Figure 8 shows two-dimensional χ^2 contours for W_0 versus R_c (only the 90% confidence level contour, shown as a dashed line, is given). The imaging data are unable to place an upper bound on the value of W_0.

4. SPECTRAL ANALYSIS

In order to test further the ability of the CFF nonpolytropic model to describe the X-ray emission from the Coma Cluster, we confront the model with spectral data in the energy range covering 0.7–20 keV obtained by the two Japanese satellites *Tenma* and *Ginga* and by the European satellite *EXOSAT*. In a series of papers over the last several years (Hughes et al. 1988b; Hughes et al. 1988a; Hughes et al. 1993), these data sets were analyzed in a consistent fashion. Since the various instruments viewed larger or smaller regions of the cluster (due to their differently collimated fields of view), it was possible to jointly analyze the data sets to discover the presence of a temperature gradient in the Coma Cluster. Larger field-of-view instruments (or off-center pointings in the case of *EXOSAT* data) consistently yielded lower best-fit temperatures when compared with smaller field-of-view instruments, leaving no doubt that the temperature variation was a global effect and that the inner parts of the cluster were hotter than the outer regions. Although the gradient was weak, it was poorly described by a polytropic model, and a phenomenological model, consisting of an isothermal core surrounded by a polytropic region, was introduced. The three sets of data were all consistent with this model and indicated an isothermal region of temperature about 9 keV extending to a radius of roughly 24′ ($\sim$1 Mpc) and decreasing beyond with a polytropic index $\gamma = 1.555$. These are by no means the possible allowed temperature distributions (see Hughes 1989 for a whole host of others), but represented merely a convenient parameterization. Other authors, Watt et al. (1992) in particular, confirm the shallowness of the temperature profile for Coma. These authors find the projected temperature distribution for Coma is nearly constant out to a radius of 30′.

We constructed a two-dimensional grid of nonpolytropic spectral models in the parameters T_0 and W_0, since these are the principal parameters for the spectral analysis. We associated each value of W_0 in the grid with the best-fit values for β, R_c, and n_0 from the imaging analysis (basically running down the middle of the dashed contour in Fig. 8). This procedure guaranteed agreement with the IPC results. Because of the large fields of view of all the spectrometers, the results are not particularly sensitive to these imaging parameters.

For each particular model in the grid of T_0 versus W_0, we employ the following procedure to generate a trial spectrum. The cluster is divided into a large number of constant temperature radial shells which are weighted by the appropriate value of $n(R)^2$, projected to the plane of the sky and convolved with the sky beam pattern of the instrument under consideration. This gives the weighting factor for this temperature value. An isothermal plasma model is calculated at each temperature and multiplied by the weighting factor. The final spectrum is the sum of the individual spectra from the various radial shells. Each instrument has its own unique beam pattern; thus, it was necessary to make a separate grid of models for each data set.

A χ^2 grid was constructed for each data set. To obtain acceptable fits to the spectral models, we need to include (and possibly vary) additional parameters, such as the metal abun-

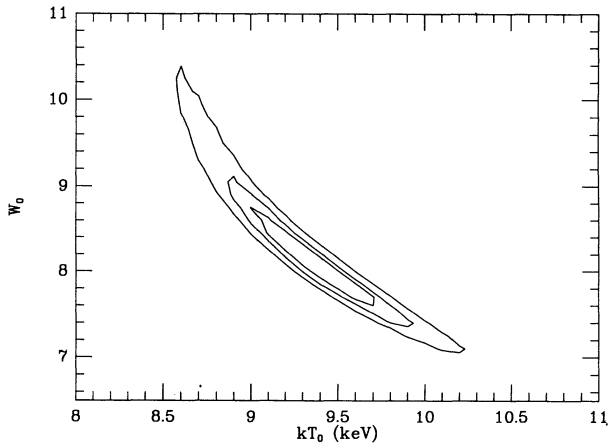

FIG. 4.—Results of the fits to the *Tenma*, *EXOSAT*, and *Ginga* spectra of Coma Cluster. Two-dimensional χ^2 contours (at the 68%, 90%, and 99% confidence levels) for W_0 vs. kT_0 using the CFF nonpolytropic model.

dance, the column density to the source, and the emission measure. We fixed the column density to a value of 3×10^{20} cm^{-2} (as for the IPC imaging analysis), but we let the other spectral parameters be free. The fitted abundance values were in the range 0.2–0.25 of solar, consistent with previous determinations.

In general, each data set by itself was able to constrain the allowed models to lie within a more or less narrow band in T_0, and placed only very weak constraints on W_0. This can be understood qualitatively by realizing that the principal action of variable T_0 in the model is to define the mean temperature for the cluster, while W_0 defines the temperature distribution. The data from these broadband collimated instruments taken individually are quite good at determining a mean cluster temperature, but rather poorer at determining the distribution. However, by adding the χ^2 grids (of T_0 vs. W_0) from the separate data sets, we are able to synthesize the information (albeit limited) on spatial variation of temperature hidden in the different pointing directions and fields of view and obtain a more encouraging result. The summed χ^2 grid is shown in Figure 4 (kT_0 vs. W_0) which gives the 68%, 90%, and 99% confidence intervals for the joint fit to all the spectral data. Table 2 provides actual numerical values for the fitted quantities. The minimum χ^2 is 1550.8 for 1482 degrees of freedom (corresponding to the 90th percentile). This must be considered excellent agreement, since we have not included contributions to χ^2 due to systematic effects such as uncertainties in background subtraction and gain calibration. This is also a considerably better fit than is obtained for a purely isothermal atmosphere, which yields an average temperature of 8.1 keV and a total χ^2 of 1580.0. From the point of view of the X-ray spectra, the CFF nonpolytropic model incorporates one additional free parameter. The *F*-test indicates that the inclusion of this free parameter is significant at greater than 5 σ confidence level.

TABLE 2

BEST-FIT SPECTRAL PARAMETER VALUES FOR COMA CLUSTER

Parameter	Nonpolytropic Model
T_0 (keV)	9.39 (+0.42; −0.47)
W_0	8.05 (+0.83; −0.63)
χ^2 (dof)	1550.8 (1482)

In Figure 5 we present the results of the spectral fitting for each data set separately in order to give the reader a sense of their relative importance. The panels show curves of χ^2 versus kT_0 for fixed best-fit values of β, R_c, n_0, and W_0. The curves then are a slice through the contour in Figure 4 at a value of $W_0 = 8.05$. The global best fit for T_0 is marked on each curve as a cross. First, one should note the excellent agreement among the data sets: the individual best-fit T_0 values are all within $\Delta\chi^2 = 2.0$ of the global best-fit T_0 value. Because of the high statistical signal and broad energy coverage, the *Ginga* data are the most constraining of T_0, while the *EXOSAT* off-center observations, which were the lowest statistical signal data of the group, are the least constraining. We stress that all the data sets are of roughly equal importance in constraining the allowed range of W_0.

Recent X-ray spectral observations (Watt et al. 1992) find that the core of the Coma Cluster is very nearly isothermal out to at least 30′. The CFF nonpolytropic model does predict a shallow temperature gradient within the central 30′ of the cluster: the projected temperature decreases from 9 keV at the center to only about 7.5 keV at 30′. We compared the projected temperature values of our best-fit model at 3′, 9′, 15′, 21′, and 27′ with the data from Figure 5 of Watt et al. (1992) and obtained a χ^2 of 9.06 for 5 degrees of freedom (corresponding to the 90% confidence level). We stress that no model parameters were adjusted in this comparison and that most of the contribution to χ^2 came from a difference in the overall temperature scale between the Watt et al. data and our model and not from the form of the temperature gradient. A more detailed analysis is beyond the scope of this work; however, given the simplicity of the comparison, we believe that this is additional supporting evidence in favor of the CFF nonpolytropic model.

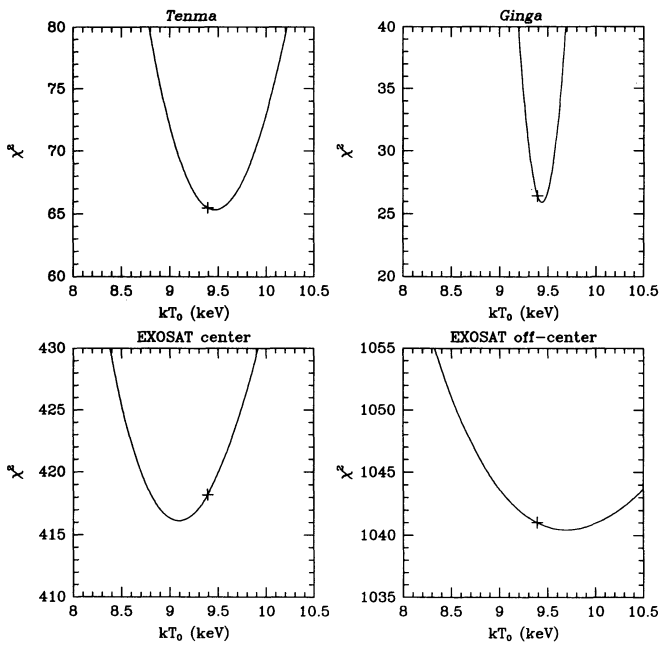

FIG. 5.—Results of the fits to the spectral data. One-dimensional χ^2 contour (90% confidence level) for the central gas temperature (T_0). The other parameter values are set to their best-fit values ($\beta = 0.644$; $R_c = 8'.1$; $W_0 = 8.05$; and $n_0 = 2.77 \times 10^{-3}$ cm^{-3}).

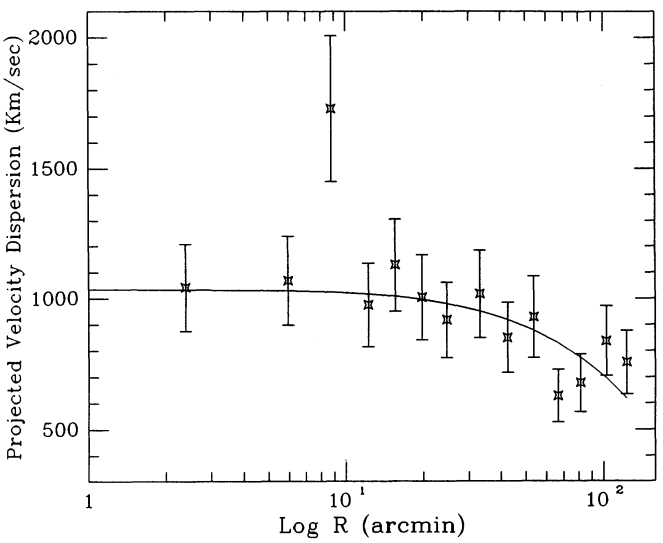

FIG. 6a

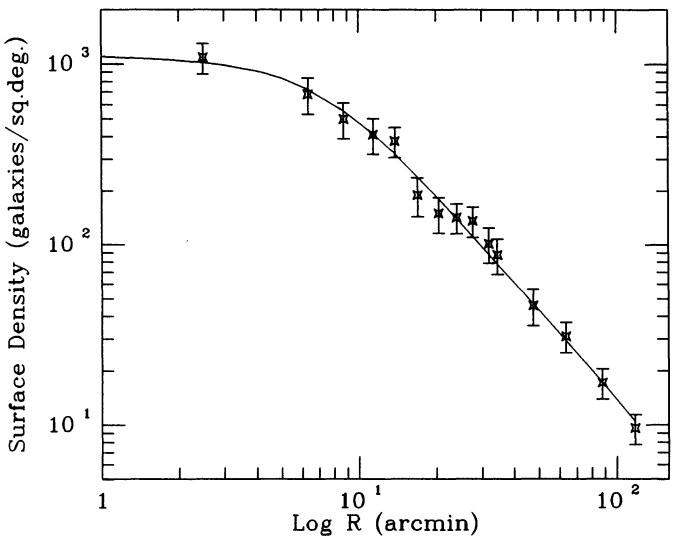

FIG. 6b

FIG. 6.—(*a*) Projected velocity dispersion and (*b*) surface galaxy density of the Coma Cluster with best-fit nonpolytropic model

5. ANALYSIS OF THE OPTICAL DATA

In this section, we intend to verify that the parameter values of the CFF nonpolytropic model derived in the preceding sections from fits to the X-ray data are consistent with the galaxy density and velocity dispersion profiles of the Coma Cluster. The & White (1986) studied these profiles starting from the data on galaxy positions and velocities published by Tifft & Gregory (1976) and Kent & Gunn (1982). The data are restricted to radii interior to 133′ because of the very strong possibility that galaxies beyond this radius are contaminated by unvirialized parts of the Coma Supercluster. The projected distributions are shown in Figures 6*a* and 6*b*, along with the best-fit nonpolytropic model; the numerical values of the fitted parameter are reported in Table 3. Note that for the optical analysis we fixed the parameters T_0 and n_0 to the values from the X-ray analysis. The central value of the velocity dispersion is given by the definition of the parameter β:

$$\sigma_0 = (kT_0\,\beta/\mu m_H)^{1/2} \simeq 1252\beta^{1/2}(kT_0/10\ \mathrm{keV})^{1/2}\ \mathrm{km\ s^{-1}}\ .$$

Using the values from Table 3, we derive $\sigma_0 = 1034(+101, -98)$ km s^{-1}.

The error intervals on some of the variable parameters in Table 3 for one or the other optical data set are poorly constrained. For example, fits to the galaxy density profile only set lower limits on the values of W_0 and β. The velocity dispersion data constrain a rather broad region in the $R_c - W_0$ plane but not the ranges of the individual values. Immediately below, we present figures which show the range of parameter space explored and the allowed regions from the fits.

Two-dimensional χ^2 contours (68% and 90% confidence level) for β versus R_c based on the velocity dispersion and surface galaxy density data are shown in Figure 7. The most stringent constraints on β and R_c are imposed by the fit to the X-ray imaging data represented by the dashed contour (this is

TABLE 3

BEST-FIT PARAMETER VALUES FOR COMA CLUSTER FROM OPTICAL DATA

Parameter	Velocity Dispersion	Galaxy Density
R_c	2′.59(...; ...)[a]	9′.00(+ 3′.22; −2′.10)
β	0.76(+ 0.16, −0.14)	1.56(...; −1.09)[a]
W_0	8.86(...; −2.00)[a]	8.78(...; −0.78)[a]
T_0 (keV)	9.00[b]	9.00[b]
n_0 ($\times 10^{-3}$ cm^{-3})	2.77[b]	2.77[b]
Σ_0 (galaxies deg^{-2})[c]	...	1094.3(+ 407.4; −410.2)
χ^2 (dof)	14.98 (11)	4.91 (11)

[a] Indeterminate error bound.
[b] Parameter held fixed at value from X-ray analysis.
[c] Central galaxy density.

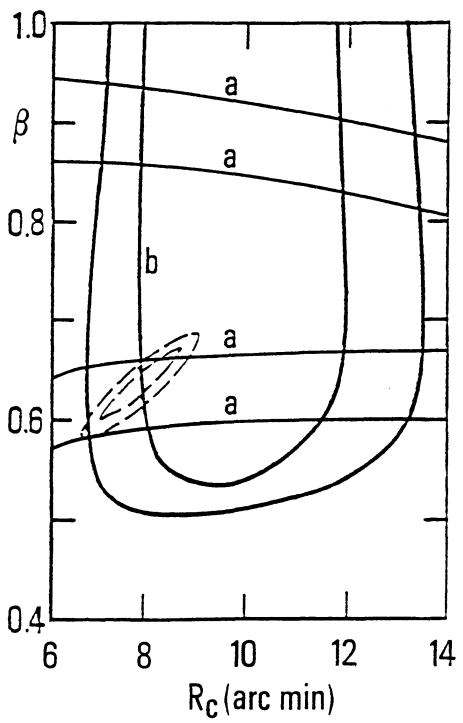

FIG. 7.—Results of fits to the projected velocity dispersion (*a*) and surface galaxy density (*b*). Two-dimensional χ^2 contours (at the 68% and 90% confidence levels) for β vs. R_c. The dashed contours are the results of the fit to the IPC data.

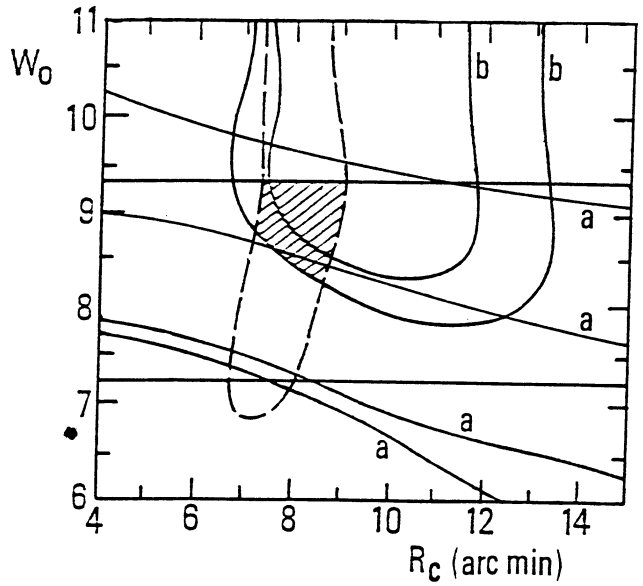

FIG. 8.—Results of the fits to the projected velocity dispersion (*a*) and surface galaxy density (*b*). Two-dimensional χ^2 contours (at the 68% and 90% confidence levels) for W_0 vs. R_c. The dashed contours are the results of the fit to the IPC data (at the 90% confidence level), while the straight lines arise from fits to the spectral data (also at the 90% confidence level). The dashed area indicates the region of overlap between the fits to the X-ray and optical data.

the same set of contours as in Fig. 3). The optical data analysis is fully consistent with this allowed region of parameter space.

The χ^2 contours (68% and 90% confidence levels) for the gravitational potential W_0 versus the core radius R_c are presented in Figure. 8 The figure-shaped dashed contour is from the X-ray imaging data for a fixed central temperature $kT_0 \sim 9$ keV, while the two horizontal lines define the allowed region from the fits to the X-ray spectral data (see Fig. 4). Both of these contours were determined at the 90% confidence level. The results of the fits to the X-ray and optical data show a large region of overlap for parameter ranges of $W_0 = 8.2$–9.3 and $R_c = 7'.3$–$9'.2$. This range is consistent with previously known values of W_0 (8.5) and R_c ($8'.5$) for the Coma Cluster (Merritt 1987). Limits on the central gas temperature are imposed by the fits to the X-ray spectral data (Fig. 4). For the allowed range of W_0 just quoted above, we find that $T_0 =$ 8.8–9.4 keV.

Additional proof that the X-ray and optical data are consistent is given by the acceptable values of χ^2 obtained when the optical data are fitted with the model parameters fixed to the best-fit values from the X-ray analysis (see Tables 1 and 2). The χ^2 values in this case are 17.25 and 12.31 for the velocity dispersion and galaxy density profiles, respectively, both for 14 degrees of freedom.

6. DISCUSSION

From the joint analysis of the X-ray and optical data, we find an acceptable fit to the CFF nonpolytropic model with the following parameter values: $\beta \equiv (0.59$–$0.68)$; $R_c \equiv (7'.3$–$9'.2)$; $W_0 \equiv (8.2$–$9.3)$; $T_0 \equiv (8.8$–$9.4)$ keV; and $n_0 \equiv (2.57$–$3.03) \times 10^{-3}$ cm^{-3}. The central velocity dispersion, σ_0, is a derived parameter based on the definition of β; we find that it lies in the interval (900–1000) km s^{-1}. In Figure 9 we show the temperature and density distributions of the intracluster gas for parameter values taken at the midpoint of the above intervals. The truncation radius of the cluster (where $\rho_G = \sigma = 0$) is ~ 15 Mpc.

The *ROSAT* all sky survey data for Coma obtained values of $\beta = 0.75 \pm 0.03$ and $R_c = 10'.6 \pm 0'.6$ from an azimuthally averaged surface brightness profile (Briel, Henry, & Böhringer 1992). In an analysis which considered the ellipsoidal shape of the X-ray emission from the Coma Cluster, Davis & Mushotzky (1993) obtained values of $\beta = 0.84 \pm 0.10$ and $R_c = 16'.3$ ($+5'.3$, $-3'.2$). These values are indeed different from those we quote above, which were obtained using the so-called north data set from the *Einstein* IPC (see the discussion at the beginning of § 3). However, as Figures 7 and 8 show, these other sets of values are fully consistent with the optical results (as represented by the contours labeled a and b), and thus our conclusions regarding the validity of the CFF nonpolytropic model remain unmodified.

Figures 10*a* and 10*b* show the integral binding and gas mass distributions and the contribution of the gas to the total virial

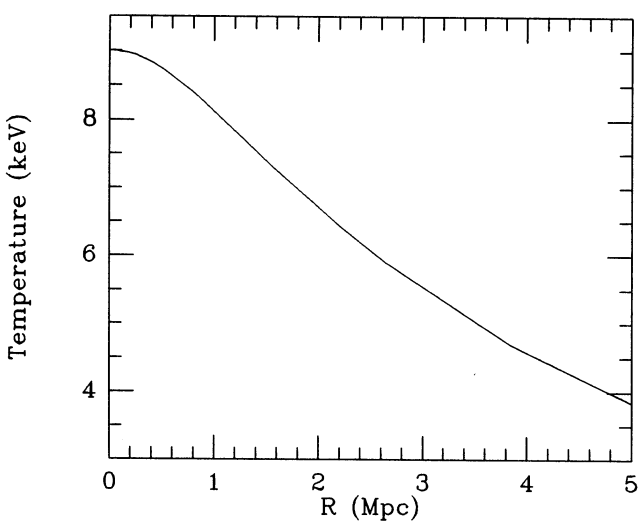

FIG. 9*a*

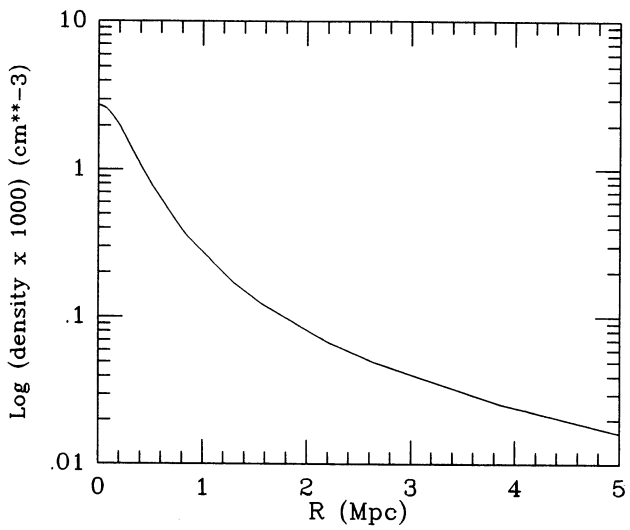

FIG. 9*b*

FIG. 9.—(*a*) Gas temperature and (*b*) density profiles of the best-fit nonpolytropic model for the combined analysis of the X-ray and optical data of Coma Cluster.

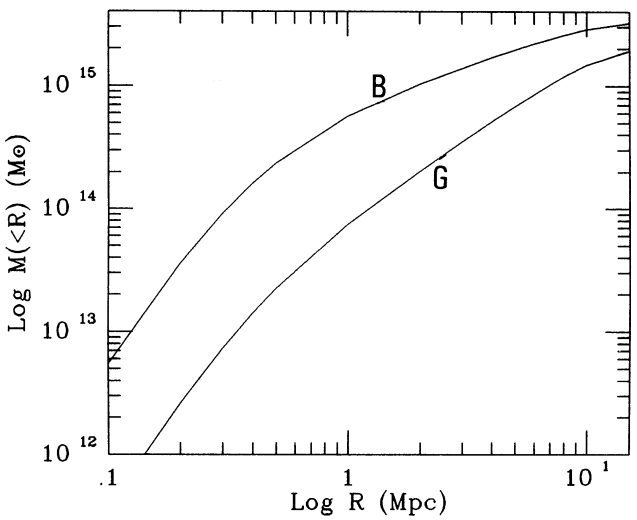

FIG. 10*a*

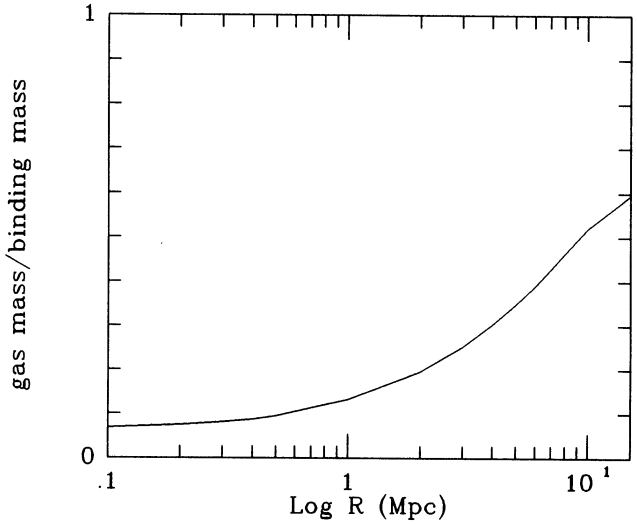

FIG. 10*b*

FIG. 10.—(*a*) Binding (B) and gas (G) mass profiles of the Coma Cluster. (*b*) Contribution of the gas to the total virial mass as a function of radius.

mass of the cluster. The total binding masses within 1 h_{50}^{-1} Mpc ($\sim$24′) and 5 h_{50}^{-1} Mpc ($\sim$122′) are $5.65 \times 10^{14}\ h_{50}^{-1}\ M_\odot$ and $1.96 \times 10^{15}\ h_{50}^{-1}\ M_\odot$, respectively. These values are in agreement with those reported by Hughes (1989) for the mass-follows-light model and more general binding mass distributions. Watt et al. (1992) quote a total cluster mass within 1 Mpc in the range $4.2\text{–}5.2 \times 10^{14}\ h_{50}^{-1}\ M_\odot$ from their X-ray spectral image of the Coma Cluster obtained with a coded mask telescope. The slight difference compared to our reported mass is mainly due to the difference between our temperature profile and the isothermal distribution used to analyze their data.

At a radius of $\sim 2\ h_{50}^{-1}$ Mpc, within which the IPC imaging X-ray data define the gas density relationship, about 20% of the binding mass may be accounted for by the intracluster gas. Beyond this radius we rely on an extrapolation of the gas density distribution based on the model fitting results. At 5 h_{50}^{-1} Mpc for the nominal parameter values, the contribution is $\sim$35%, clearly within the range 16%–53% estimated by Hughes (1989). Varying the values of the parameters R_c, W_0, and T_0 through their allowed ranges introduces a negligible variation of this value. On the other hand, a more significant change arises from variation of the value of β; smaller β values will increase the relative contribution of the gas to the total binding mass. For example, for $\beta = 0.63$ the gas to binding mass ratio (at ratio (at 5 h_{50}^{-1} Mpc) increases to $\sim$44%. To better define this quantity requires imaging data to large radii and spatially resolved X-ray spectra.

The CFF nonpolytropic model gives mass-to-light ratios of $157\ h_{50}\ M_\odot/L_\odot$ and $163\ h_{50}\ M_\odot/L_\odot$ within 1 h_{50}^{-1} Mpc and 5 h_{50}^{-1} Mpc, respectively, where we have assumed total (deprojected) blue luminosities of $0.36 \times 10^{13}\ h_{50}^{-2}\ L_\odot$ (1 h_{50}^{-1} Mpc) and $1.2 \times 10^{13}\ h_{50}^{-2}\ L_\odot$ (5 h_{50}^{-1}) Mpc (from Kent & Gunn 1982; see Hughes 1989).

7. CONCLUSIONS

As we have shown in this paper, the nonpolytropic model originally formulated by CFF is fully consistent with the density and temperature distributions of the gas and galaxies in the Coma Cluster. The principal assumption of this model is that the ratio of the temperatures of the gas and the galaxies is constant throughout the cluster. If gravitational collapse were the only source of energy input to the gas and galaxies, then one would expect the ratio of these temperatures (i.e., β) to be unity. In our fits to the Coma data presented here, we determine a best-fit value of $\beta = 0.64$. Others (Briel et al. 1992; Davis & Mushotzky 1993) have obtained β values in the range 0.75–0.84.

As numerous authors have pointed out (Jones & Forman 1984; White 1991; David, Forman, & Jones 1991), values of β less than unity require an additional source of energy input to the gas (or a mechanism for cooling the galaxies). White (1991) has studied the energetics associated with metal enrichment of the intracluster medium and considered energy input from ram pressure stripping and galactic winds (see also David et al. 1991). He shows that while the energy input from gas stripping processes enters as σ^2 (as we also state in § 2 above), energy input from galactic winds depends on the depth of the potential well of the individual galaxy, as well as the wind speed, and not only on σ^2. However, for rich massive clusters (like Coma) the effects of galactic winds on the energetics of intracluster gas may be marginal ($\sim$10%), merely because the average galaxy velocity through the cluster is so much higher than the average galaxy wind velocity.

The validity of the CFF nonpolytropic model (given the current X-ray and optical data) suggests that a significant fraction of the thermal energy contained in the hot gas in the Coma Cluster may have become from the ram pressure stripping of galaxies by the ambient cluster medium. This should also be the situation for other rich galaxy clusters, while less massive systems should show more evidence for the collective effects of winds from individual galaxies. We look forward to the imminent arrival of greatly improved X-ray data on clusters of galaxies from *ASCA* (*Astro D*), which should allow us to begin discriminating among the various scenarios for the sources of energy input to and transport within the hot intracluster gas of clusters of galaxies.

This work was partially supported by funds from the Smithsonian Institution and the Instituto di Astrofisica Spaziale. J. P. H. also acknowledges support from NASA grants NAG8-699 and NAG 8-181. We appreciate Larry David's careful reading of the manuscript.

REFERENCES

Abramopoulos, F., & Ku, W. H. 1983, ApJ, 271, 446
Avni, Y. 1976, ApJ, 210, 642
Blumenthal, G. R., Faber, S. M., Primack, J. R., & Rees, M. J. 1984, Nature, 311, 517
Branduardi-Raymont, G., Fabricant, D., Feigelson, E., Gorenstein, P., Grindlay, J., Soltan, A., & Zamorani, G. 1981, ApJ, 248, 55
Briel, U. G., Henry, J. P., & Böhringer, H. 1992, A&A, 259, L31
Cavaliere, A., & Fusco-Femiano, R. 1976, A&A, 49, 137
———. 1978, A&A, 70, 677
———. 1981, A&A, 100, 194 (CFF)
David, L. P., Arnaud, K. A., & Forman, W., & Jones, C. 1990, ApJ, 356, 32
David, L. P., Forman, W., & Jones, C. 1991, ApJ, 380, 39
David, L. P., Hughes, J. P., & Tucker, W. H. 1992, ApJ, 394, 452
Davis, D. S., & Mushotzky, R. F. 1993, AJ, 105, 409
De Young, D. S. 1978, ApJ, 223, 47
Giacconi, R., et al. 1979, ApJ, 320, 540
Gorenstein, P., Fabricant, D., Topka, K., Harnden, F. R., Jr., & Tucker, W. H. 1978, ApJ, 224, 718
Gull, S. F., & Northover, K. J. 1975, MNRAS, 173, 585
Hughes, J. P. 1989, ApJ, 337, 21
Hughes, J. P., Butcher, J. A., Stewart, G. C., & Tanaka, Y. 1993, ApJ, 404, 611
Hughes, J. P., Gorenstein, P., & Fabricant, D. 1988a, ApJ, 329, 82
Hughes, J. P., Yamashita, K., Okumura, Y., Tsunemi, H., & Matsuoka, M. 1988b, ApJ, 327, 615
Jones, C., & Forman, W. 1984, ApJ, 276, 38
Kent, S. M., & Gunn, J. E. 1982, AJ, 87, 945
Kent, S. M., & Sargent, W. L. 1983, AJ, 88, 697
King, I. R. 1966, AJ, 71, 64
Lampton, M., Margon, B., & Bowyer, S. 1976, ApJ, 208, 177
Larson, R. B., & Dinerstein, H. L. 1975, PASP, 87, 911
Lea, S. M. 1975, ApJ, 16, L141
Merritt, D. 1987, ApJ, 313, 121
Mitchell, R. J., & Culhane, J. L. 1977, MNRAS, 178, 75p
Mitchell, R. J., Culhane, J. L., Davison, P. J., & Ives, J. C. 1976, MNRAS, 176, 29p
Raymond, J. C., & Smith, B. W. 1977, ApJS, 35, 419
Rood, H. J., Page, T. L., Kintner, E. C., & King, I. R. 1972, ApJ, 175, 627
Serlemitsos, P. J., Smith, P. W., Boldt, E. A., Holt, S. S., & Swank, J. H. 1977, ApJ, 211, L63
The, L. S., & White, S. D. M. 1986, AJ, 92, 1248
Tifft, W. G., & Gregory, S. A. 1976, ApJ, 205, 696
Watt, M. P., Ponman, T. J., Bertram, D., Eyles, C. J., Skinner, G. K., & Willmore, A. P. 1992, 258, 738
White, R. E., III. 1991, ApJ, 367, 69